Principles of smart (self-controlled) structures development

The head of scientists teams

Professor Gela Kipiani

Secretary-General of the Georgian National Committee
of Theoretical and Applied Mechanics
Full Professor of the Department of Engineering Mechanics
of Georgian Technical University
M.Kostava 77
TBILISI 0175
GEORGIA

.

gelakip@mail.ru

gelakip@gmail.com
Tel : +995 32 2371984 (office)
+995 32 2342571 (home)
+995(8)599 106263 (mob)

1. *Essence of the Project and its Scientific Value*

1.1 Purpose of the project, tasks to be accomplished for each stage and indicators of the expected results

In 1980-ies the study of complex structures mainly starts on the basis of executed in the space works. Was expressed the opinion that it would be better to install in spacecraft the "central nervous system" that, roughly speaking, would be the simulation of human's nervous system. Although the main aspects of space equipment's and structures sensitivity was studied the main accent were made on carbon-epoxy panels and similar composite materials. In the composite panels will not be used conventional methods of survey and sensing that are traditionally used in metal structures. It was necessary to define the operability of such composite panels. Also is necessary to raise the issue of hazard detection and on methods of report of operating personnel or equipment.

In parallel with mentioned studies is carried out development of smart (fiber-optic and electromechanical) sensors with application of up-to date opto-electronic achievements.

In our opinion is necessary to develop the “structure- smart sensor-drive” system as integrated part that would be adapted to environmental conditions, would be autonomous and protected from possible hazards.

The objective of work is to develop the principles of smart structures creation and automatic control system development.

The topicality of problem largely is reflected in the fact that developed in the project smart (self-controlled) structures are very attractive and applicable in having risk responsible facilities in aerospace industry as well as in bridges, dams, tower buildings, television towers, and others to undergoing the unexpected forces impact. Let’s recall the case of 2011 earthquake and tsunami in Japan that failed in awful state such responsible facilities as nuclear power stations, high-voltage transmission lines, tower building etc.

From the preliminary analysis of patent search is clear that developed by group of authors universal system of self-controlled structures are distinguished by unique design and hardware and software. Such systems nowadays haven’t analogues in the world.

The lot of theoretical and practical solutions is known in this field that is attached to the presented project.

The novelty of study consists in development due the modern approach such “structure- smart sensor-drive” system on the basis of existing ones that provides the adaptation, protection and state assesment of structure.

The ground of project’s development is the acquisition by authors of Georgia patents 1173, 3415, 3416, 1107 and published in 2009 in Boston, USA the monograph: Controlled Structures with Electromechanical and Fiber-Optical Sensors.

The fragments of study of system that would be developed by authors are given below:

Regulation of operation of combined framed structures using electromechanical and fiber-optic sensors

There are several types of frame straining devices including those using hoist and planetary reduction gears. The diagrams of their application are given in Fig. 1 and 2. In the carried out experiments the planetary gearboxes were used.

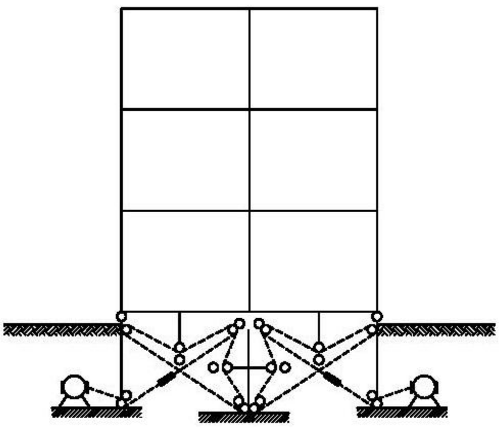

Fig. 1. Diagram of hoist usage.

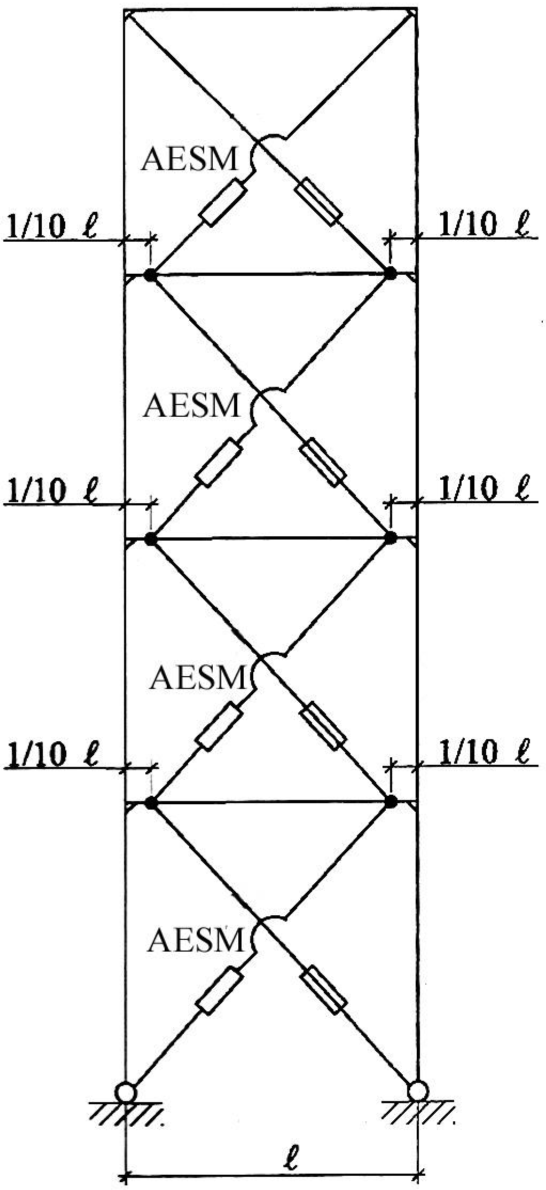

Fig. 2. Diagram of using of planetary reducer.

Automatic regulation of seismic load for metal frames

Theoretical and experimental researches were executed on a frame model (see Fig. 3).

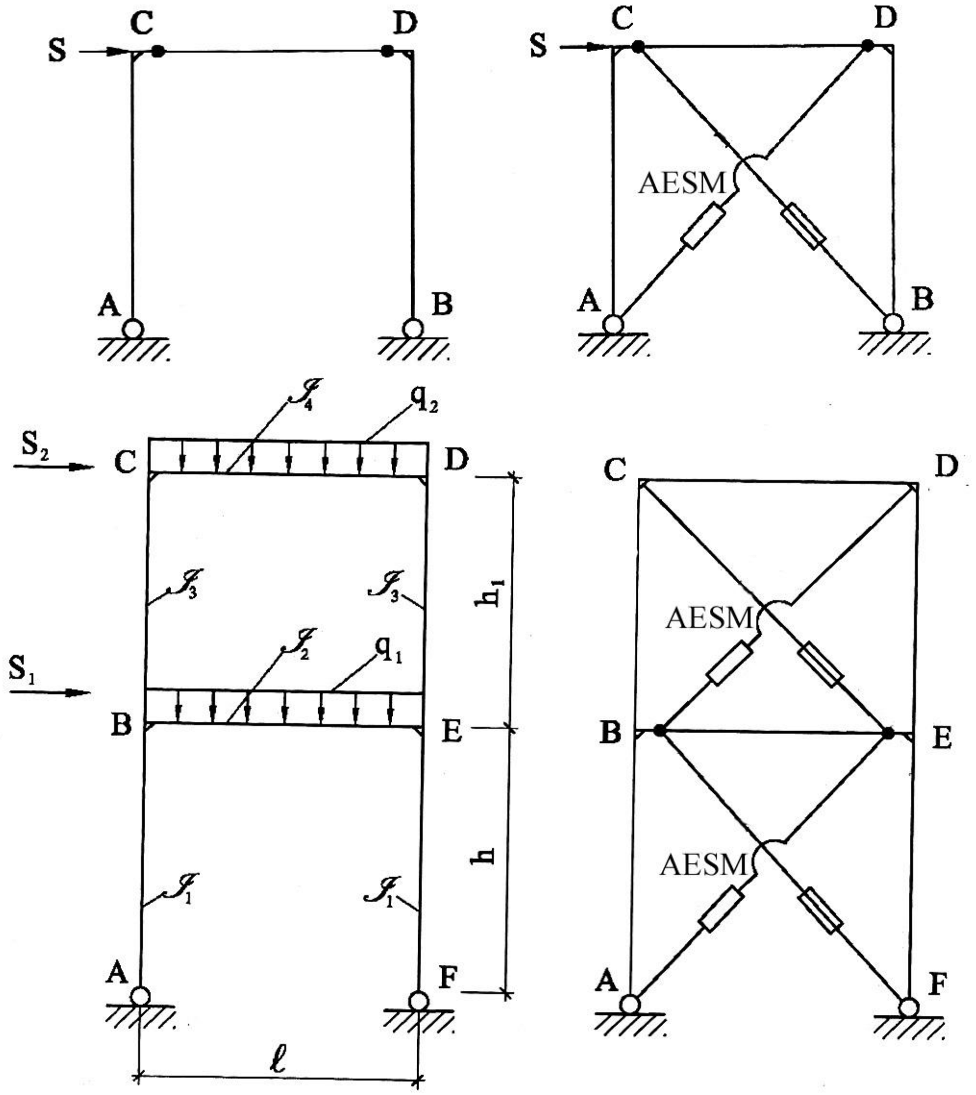

Fig. 3. Frame models used in researches

Model one. Single span one storey open contour frame was made from pipes. Pipe diameter was 32.5 mm, frame span ℓ= 680 mm, height h = 1240 mm. On one diagonal tie-bar with diameter 2.2 mm a planetary gearbox with electric drive and a relay with contactors were instaled.

The second model had the same geometrical dimensions and cross-sections, except the lower collar beam support added in the distance of 150 mm which made closed contour of the frame (Fig. 4).

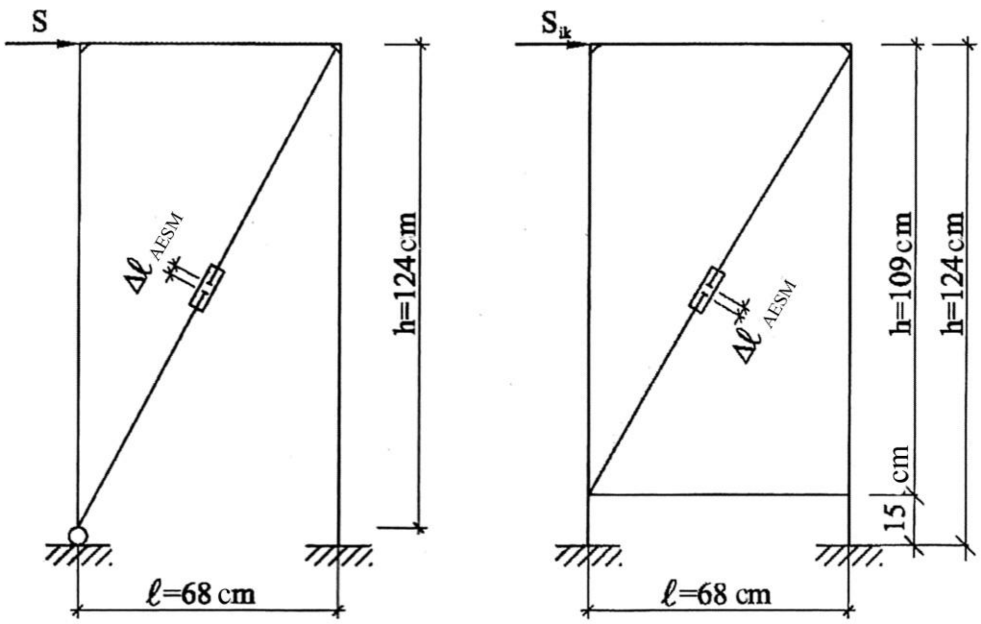

Fig. 4. Closed contour frame.

As it is known horizontal seismic force S_{ik} is determined with the product of many coefficients including dynamic coefficient β_i which depends on the period of frame natural vibration and on its variation. Seismic loads may be regulated 2 ÷ 2.5 times.

In order to include AESM into frame operation it is necessary to preliminary define gap between AESM relay contactors which is determined by formula:

$$\Delta\ell_{AESM} = (T + \Delta T)\left(\frac{\ell_{cont}}{E_{cont}F_{cont}} - \frac{\ell_{cobl}}{E_{cobl}F_{cobl}}\right) \quad (1)$$

or

$$\Delta\ell_{AESM} = \frac{S_{ik}}{K_i}(i_{cont} - \ell_{cobl}); \; k_i = \frac{S_{ik}}{(T + \Delta T)} \quad (2)$$

where T is prestrain in cable (in diagonal bracing);

S_{ik} is seismic force;

Δ T is cable (diagonal bracing) selfstressing force;

l_{cont} is the length of contactor spring and cable including AESM;

E_{cont} F_{cont} is the stiffness of contactor spring and cable including AESM;

ℓ_{cabl} is cable (diagonal bracing) length without AESM;

E_{cabl} F_{cabl} is cable (diagonal bracing) stiffness without AESM.

Here E_{cont}, E_{cabl}, $F_{cont,}$ and F_{cabl} are respective modulus of elasticity and cross-section areas of contactor spring and cable.

For determination of coefficient K_i three calculations and tests have been carried out.

The first calculation is based on classical method of forces according to which the mentioned frame models represent, in one case, 4 times statically indeterminable and, in the second case, 7 times statically indeterminable systems (Fig. 5).

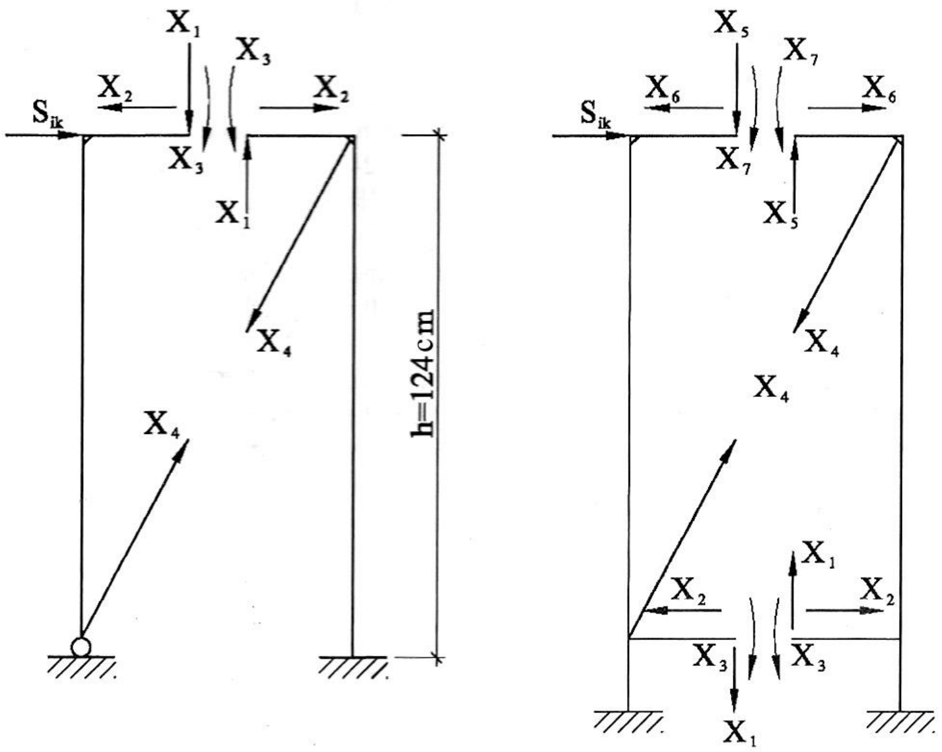

Fig. 5. Statically indeterminate systems.

As a result of testing an open contour frame we get that when strain in diagonal bracing cable was T+ ΔT = 29.3 kg (0.293 kN), in case of horizontal static load S_{ik} = 175 kg (1.75 kN), the upper joint of frame collar-beam was displaced for f = 23.6 mm. After switching in of AECM displacement made f = 24.6 mm, strain in cable decreased and became T+ ΔT=16 kg (0.16 kN). In this case coefficient K_i = 5.97.

Three calculations were done for the second, closed contour frame by method, as was mentioned above, of forces using program "SAP-2000 Student" and program "LIRA".

The canonical equation in matrix expression will be:

$$X_i \cdot \Delta = \vec{\Delta}_p \tag{3}$$

The equation can be written in the following form when S_{ik} =1:

$$i = \begin{Vmatrix} x_1 \\ x_2 \\ x_3 \\ x_4 \\ x_5 \\ x_6 \\ x_7 \end{Vmatrix}; \; \Delta = \begin{Vmatrix} 0,061 & 0 & 0 & -0,027 & 0,035 & 0 & 0 \\ 0 & 0,002 & -0,023 & -0,007 & 0 & 0,027 & -0,023 \\ 0 & -0,023 & 0,980 & 0,089 & 0 & -0,349 & 0,300 \\ -0,027 & -0,007 & 0,089 & 0,147 & -0,124 & -0,312 & 0,374 \\ 0,035 & 0 & 0 & -0,124 & 0,313 & 0 & 0 \\ 0 & 0,027 & -0,349 & -0,312 & 0 & 1,271 & -1,538 \\ 0 & -0,023 & 0,300 & 0,374 & 0 & -1,538 & 3,160 \end{Vmatrix}; \vec{\Delta}_p = \begin{Vmatrix} -0,059 \\ 0,013 \\ -0,175 \\ -0,006 \\ -0,261 \\ 0,636 \\ -0,769 \end{Vmatrix} \tag{4}$$

Square matrix of order 7 is reduced to that of order 5 and is solved using "MATCAD".

$$A:=\begin{pmatrix} 0,002 & -0,023 & -0,007 & 0,027 & -0,023 \\ -0,023 & -0,98 & 0,089 & -0,349 & 0,300 \\ -0,022 & 0,274 & 0,308 & -0,974 & 1,153 \\ 0,027 & -0,349 & -0,312 & 1,271 & -1,538 \\ -0,023 & 0,300 & 0,374 & -1,538 & 3,160 \end{pmatrix};$$

$$\text{b}:=\begin{pmatrix} 0,013 \\ -0,175 \\ -0,326 \\ 0,636 \\ -0,769 \end{pmatrix};\ \text{lsolve(A,b)}=\begin{pmatrix} 255,08X10^{-3} \\ 3,31X10^{-3} \\ 2,35X10 \\ 1,08X10 \\ 5,28X10^{-3} \end{pmatrix} \quad (5)$$

In experiments carried out for stating the relation of horizontal force S_{ik} and of tension T+ ΔT in diagonal cable, S_{ik} = 50, 100 and 150 kg (0.5, 1.0 and 1.5 kN), as well as, T = 0, 20, 30, 40 and 50 kg (0, 0.2, 0.3, 0.4 and 0.5 kN) were varied. Their relation is expressed by coefficient K_i given in Table 1.

Table 1.

Coefficient $K_i = S_{ik}/(T+\Delta T)$

Research method	S_{ik} kg T + ΔT	1 kg	50 kg	100 kg	150 kg	K_1	K_2	K_3	K_4	K average	Note
Method of forces	T + ΔT	2,33kg	117,4kg	234,9kg	352,3kg	0,43	0,43	0,43	0,43		K_1 K_2 K_3 K_4 are numeration acoording S_{ik} loads
SAP-2000 Student	T + ΔT	1,24kg	60,0kg	130,0kg	190,0kg	0,80	0,83	0,77	0,53	0.735	In determination of K average value the result of test in case of preunstrained cable is not considered, T = 0
“LIRA”	T + ΔT	2,0kg	90kg	180,0kg	270,0kg	0,50	0,55	0,55	0,55		
Test (T + ΔT) kg	T=0	-	10,0kg	12,0kg	18,0kg	-	5,0	8,33	8,33		
	T=20kg	-	44,0kg	82,0kg	127,0kg	-	1,13	1,22	1,18		
	T=30kg	-	62,0kg	104,0kg	146,0kg	-	0,80	0,96	1,03		
	T=40kg	-	78,0kg	122,0kg	163,0kg	-	0,64	0,82	0,92		
	T=50kg	-	88,0kg	136,0kg	180,0kg	-	0,57	0,74	0,83		

As is seen from the Table the relation between external horizontal force S_{ik} and tension in diagonal cable is ambiguous and is closer to the results of calculations when pretension in the cable is higher. (T+ΔT) $=S_{ik}/0.735=1.36\ S_{ik}$ can be taken as an average value necessary for stating the initial magnitude ($\Delta\ell_{AESM}$) of the gap between contactors.

Dynamic load in frame is induced with electric engine. Before switching in of automatic tie-coupling (AESM) the vibration amplitude was 1.5 mm, after switching in of AESM it was 0.5 mm.

In this case the efficiency of automatic straining tie-coupling was n_{eff} = 3.0; gap between contactors was $\Delta\ell_{AESM}$ = 10 mm.

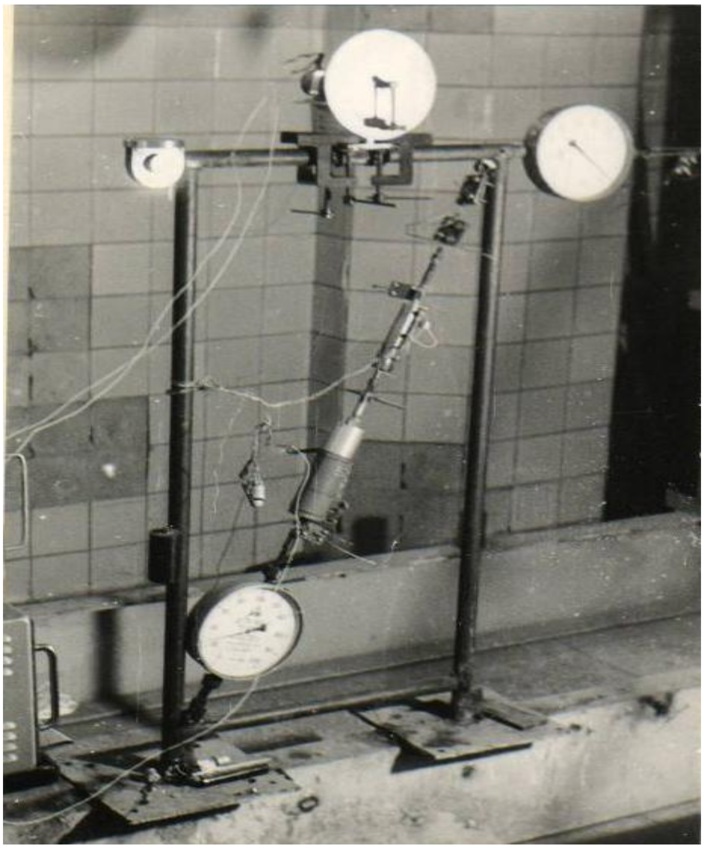

Fig. 6. View of experimental steel frame with diagonal bracing.

Vibration damping in frames using Moon beam

Cantilever rod suspended on frame collar-beam, as a result of magnetic pull in the middle of span is stretched, bended and deviated from vertical.

As a result of magnets attraction the stretching force in the bar according to Hook's law is:

$$N = \frac{\Delta l}{l} EF \tag{6}$$

The length of the bar arc deviated from vertical is defined with expression:

$$L = \int_0^1 \sqrt{1 + \left(\frac{dy}{dx}\right)^2}\, dx \tag{7}$$

Hence bar elongation equals:

$$\Delta l = L - l = \frac{1}{2}\int_0^{\ell} \left(\frac{dy}{dx}\right)^2 dx \tag{8}$$

Then stretching force in the bar will get the following expression:

$$N = \frac{EF}{l} \cdot \frac{1}{2}\int_0^{\ell} \left(\frac{dy}{dx}\right)^2 dx \tag{9}$$

The static equation of stretched-bended bar will be:

$$EI \cdot \frac{d^4 y}{dx^4} - N\frac{d^2 y}{dx^2} = q \tag{10}$$

According to d'Alembert principle the bar movement equation may be written as:

$$m\frac{\partial^2 y}{dt^2} + EI \cdot \frac{d^4 y}{dx^4} - N\frac{d^2 y}{dx^2} = B(x,t) \tag{11}$$

Here the notations are:

m is linear mass of the bar;

EI is bar stiffness;

B(x,t) is magnets effect on the bar;

EF is bar tensional stiffness;

l - is bar length.

The solution of the equation can be presented as:

$$y(x,t) = W(x)T(t) \tag{12}$$

Substituting into the equation we get:

$$EI\frac{d^4W}{dx^4}Wdx\cdot T(t) + m\int_0^\ell Wdx\frac{d^2T(t)}{dt^2} - \frac{1}{2}\frac{EF}{\ell}\int_0^\ell\left[\frac{dW}{dx}T(t)^2dx\right]\times$$
$$\times\frac{d^2W}{dx^2}Wdx = B(x,t)\int_0^\ell Wdx \tag{13}$$

Introduce notations:

$$\tilde{R}_{1x} = EI\int_0^\ell\frac{d^4W}{dx^4}Wdx;\quad R_{2x} = EI\int_0^\ell\frac{d^2W}{dx^2}Wdx;\quad R_{7x} = \int_0^\ell Wdx \tag{14}$$

Then motion equation for arbitrary external load will have the form:

$$T(t)R_{1x} + \frac{d^2T(t)}{dt^2}R_{5x} - \frac{EF}{2\ell}\tilde{R}_{1x}R_{2x}T^3(t) = B(x,t)R_{7x} \tag{15}$$

Consider magnets effect on the bar.

Unit length of the beam is acted upon with:

$$q = F_1 - F_2 = k_1\Phi_0^2/\left(a-y\right)^2 - k_1\Phi_0^2/(a+y)^2 \tag{16}$$

or

$$q = k_1\Phi_0^2/\left(a^2-2ay+y^2\right) - k_1\Phi_0^2/\left(a^2+2ay+y^2\right) = k_1\Phi_0^2\frac{\left(a^2-2ay+y^2-a^2-2ay-y^2\right)}{\left(a^2-2ay+y^2\right)\left(a^2+2ay+y^2\right)} =$$
$$= \frac{4a^2yk_1\Phi_0^2}{\left(a^2-2ay+y^2\right)\left(a^2+2ay+y^2\right)} \tag{17}$$

At small vibrations we have:

$$q = \frac{4k_1\Phi_0^2}{a^3}y \tag{18}$$

Static uniform magnetic field with constant stress of magnetic flow Φ_0 is acting on the bar.

At bar deviation from vertical line the forces that act on it are caused by different magnetic fields and their difference does not equal zero.

Magnet attraction force between N and S poles is directly proportional to the square of magnetic flux Φ_0 and inversely proportional to the square of distance between magnets.

$$\Delta F = F_2 - F_1$$
$$F_1 = k_1\Phi_0^2/\left(a-y\right)^2;\quad F_2 = k_1\Phi_0^2/\left(a-y\right)^2 \tag{19}$$

or

$$F_{1,2} = k_1\Phi_0^2/\left(a\mp y\right)^2 \tag{20}$$

Attractive forces acting on the bar placed between magnets are inter-compensated.

In the right part of vibration equation substitute $B(x,t)R_7$ with

$$q = \frac{4k_1\Phi_0^2}{a^3}y.$$

We get:

$$m\frac{\partial^2 y}{dt^2}+EI\cdot\frac{d^4 y}{dx^4}-N\frac{d^2 y}{dx^2}-\frac{4k_1\Phi_0^2}{a^3}y=0 \tag{21}$$

Find the solution in the following form:

$$y(x,y)=W(x)T(t) \tag{22}$$

Inserting in equation and using Bubnov-Galerkin method we get:

$$\frac{d^2T(t)}{dt^2}\int_0^\ell mW^2dx+T(t)\int_0^\ell E\Im\frac{d^4W}{dx^4}-T(t)\int_0^\ell N\frac{d^2W}{dx^2}-T(t)\int_0^\ell N\frac{4k_1\Phi_0^2}{a^3}W^2dx=0 \tag{23}$$

Inserting y(x,t) into $N=\frac{EF}{l}\cdot\frac{1}{2}\int_0^\ell\left(\frac{dy}{dx}\right)^2dx$ we get:

$$N=\frac{EF}{l}\cdot\frac{1}{2}\int_0^\ell\left(\frac{dw}{dx}\right)^2T^2(t)dx \tag{24}$$

Then

$$\frac{d^2T(t)}{dt^2}R_5-T(t)\left[\int_0^\ell\frac{4k\Phi_0^2}{a_1^3}W^2dx-\int_0^\ell EI\frac{d^4W}{dx^4}W\ dx\right]-T(t)T^2(t)\times$$
$$\times\int_0^\ell\left[\frac{1}{2}\frac{EF}{l}\int_0^\ell\left(\frac{dW}{dx}\right)^2dx\right]\frac{d^2W}{dx^2}Wdx=0 \tag{25}$$

or

$$\frac{d^2T(t)}{dt^2}-\omega^2T(t)+\gamma T^3(t)=0$$

We get Duffing equation where:

$$\omega^2=\frac{\left[\int_0^\ell\frac{4k\Phi_0^2}{a_1^3}W^2dx-\int_0^\ell EI\frac{d^4W}{dx^4}W\ dx\right]}{\int_0^\ell mw^2(x)dx}$$

$$\gamma=\frac{\int_0^\ell\left[\frac{1}{2}\frac{EF}{l}\int_0^\ell\left(\frac{dW}{dx}\right)^2dx\right]\frac{d^2W}{dx^2}Wdx}{\int_0^\ell mW^2(x)dx}$$

Magnetic device of Moon beam

Forced vibrations of bended cantilever beam located in the strong field of two magnets can be adequately described with Duffing nonlinear differential equation.

For Moon beam operation a magnetic device is necessary. The suspended Moon rod is placed between two magnetic beams.

Attractive force of constant electromagnet is:

$$P_3=\frac{(\bar{I}N)^2 4\pi10^{-7}}{2}\frac{S_\delta}{\delta^2}(N) \tag{26}$$

Gap between two electromagnetic beams is: δ=0,5m=50sm;

Design attractive force is: P=1t=1000kg=10000N;

Coil number on beam winding is: N = 2353 coils;

$\overline{I}$ is total current in winding.
Hence:

$$\overline{I} = \frac{2P_э\delta^2}{4\pi 10^{-7}\omega^2 S_\delta}\text{ A} \qquad (27)$$

S_δ is gap area – electromagnet cross-section;

Wires of 20.8 layers on the beam with 112,6 coils in each layer make approximately 4700 m.

Beam height is 112.6 x 4.44 = 499.9 = 500 mm.

A projection of 2 x 250 = 500 mm is added to beam height.

The total height of the beam is 1000 mm.

We received 1500 mm. Minu suspended magnetic bar is placed in partition of double layer panels, electromagnets are arranged in basement (Fig. 7).

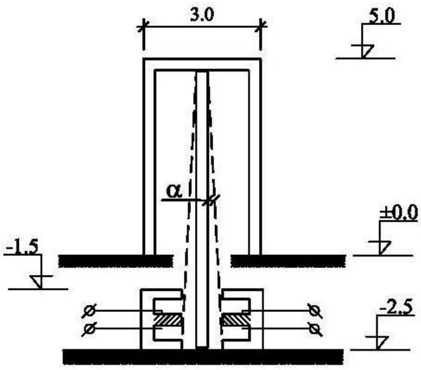

Fig. 7. Frame diagram with Moon beam.

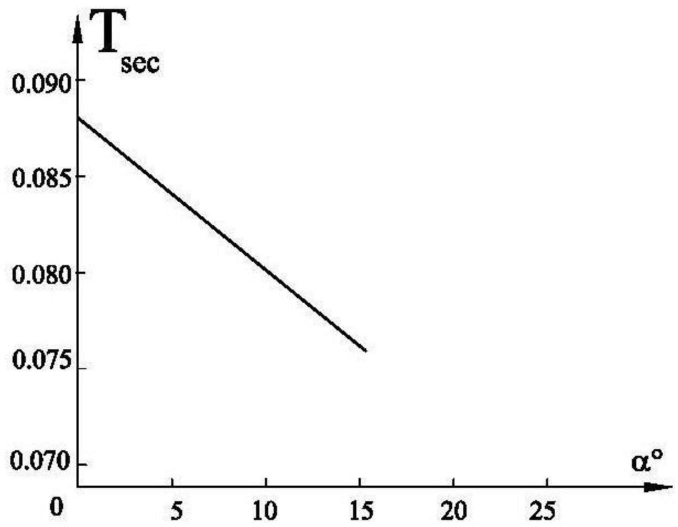

Fig. 8. The relation of frame natural vibration period to Moon beam deviation angle.

Frame span L=3.0 m; frame height H=5.0 m; frame columns and collar-beams with pipe section diameter - 140 mm; wall thickness - 40 mm; Moon suspended beam of strip steel is of 100 mm width and 20 mm thickness; cross-section area A=20 cm^2.

Cantilever beam linear mass is:

$$m = \frac{q}{g} = \frac{10\cdot 2\cdot 7,81}{9,81} = 0,167 \text{ grsec}^2\text{/cm=0,000167 kgsec}^2\text{/cm}$$

E =210000 kg/cm^2 is a design resistance in stretching and bending plane:

$$I = \frac{bh^3}{12} = \frac{10\cdot 2^3}{12} = 6,67cm^4$$

$$S_\delta = 1,5X1,5 = 0,75m$$

Insert numerical data:

$$\overline{I} = \sqrt{\frac{2\cdot 10000\cdot 0,5^2\cdot 10^7}{4\cdot 3,14\cdot 2353^2\cdot 0,75}} = 30,9Amp \approx 31Amp$$

Wire area:

$$S = \frac{31}{2} = 15,5mm^2$$

Wire diameter:

$$d_m^2 = \frac{4\cdot 15,5}{3,14} = 19,74;\ \ \mathrm{d}_m = 4,44mm$$

Circular core diameter or rectangular side's perimeter of beam is:

$$a = 0,5X4 = 2,0 = 2000mm.$$

Perimeter of circular core coil:

$$a = 2\pi R = 6,28\cdot 0,25 = 1,57m = 157mm.$$

Better take rectangle sides as a = b = 0.5 m.

$$\sum l = 2000\cdot 2353 = 4,706\cdot 10^6 mm.$$

Conductor resistance by formula is:

$$R = \rho\frac{\sum l}{S} = \frac{1,7\cdot 10^{-5}\cdot 10^6}{15,5} = 5,16ohm.$$

Here $\rho = \frac{1}{\gamma}$ is resistivity of a conductor;

γ is electrical conductance of material;

S is conductor cross-section.

Moon beam natural vibrations frequency in magnetic field is defined with formula:

$$\omega^2 = \frac{4k\Phi_0^2}{a^3 m} - \frac{12,52EI}{ml^4} \quad (28)$$

where

$$\Phi_0 = \frac{\overline{I}N}{a} = \frac{31\cdot 2353}{a} = 729,43.$$

Here $\overline{I}$ is current force equal to 31 A;

N is number of coils equal to 2353;

α - the distance from the conductor to field point is equal to 100 cm.

Then

$$\omega^2 = \frac{4\cdot 1\cdot 532068 = 12}{100^3\cdot 0,00016} - \frac{14\cdot 10^6\cdot 12 = 52}{750^4\cdot 0,00016} = 13298,24$$

ω=115.3 rad/sec; ω= 18.36 Hz.

Moon beam nonlinearity coefficient is:

$$\gamma = 6,91\frac{EF}{ml^4} = 6,91\frac{2100000\cdot 20}{0,00016\cdot 750^4} = 5,73$$

Then Moon beam differential equation of Duffing type will be:

$$\frac{d^2T(t)}{dt^2} - 18,36^2 T(t) + 5,73T^3(t) = 0$$

Stiffness in case of bending EI=2100000·6,67=14·10^6kgcm^2;

Stiffness in case of stretch EA=2100000·20=42·10^6kg;

Length of suspended beam L=750cm=7,5m.

Moon beam Duffing equation was solved according to the following rounded off initial data in program "MATCAD Professional":

$$\frac{d^2}{dt^2}x(t) + c\frac{d}{dt}x(t) - wx(t) + rx^3(t) = A \cdot \cos(\omega t) \tag{29}$$

where c =0.5

$\omega = 0$

A = 0

r=6.0

w=18.0

Phase picture is received as a result of Duffing equation solution (Fig. 9). Fig 3.8 also gives the relation of frame natural vibration period to Moon bean angle deviation.

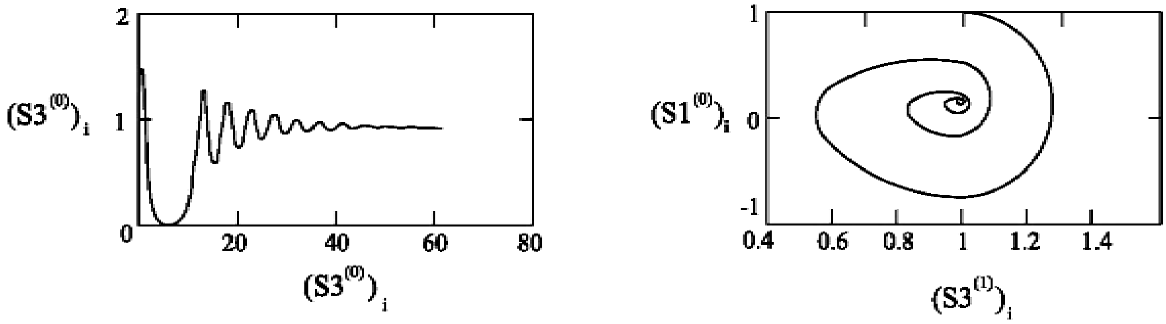

Fig. 9. Phase picture of vibrations of the frame with Moon beam.

As a conclusion we can note that using of Moon beam for vibrations damping is quite possible in particular conditions. Natural vibration period for the frame changes by linear law according to Moon beam deviation angle. According to phase trajectory the maximum rate of vibrations is:

$V_{max}=Y_{max}\cdot\omega=1,464\cdot18=26,3$ cm/sec

This problem is solved with MATCAD program. The solution is given in Fig. 10.

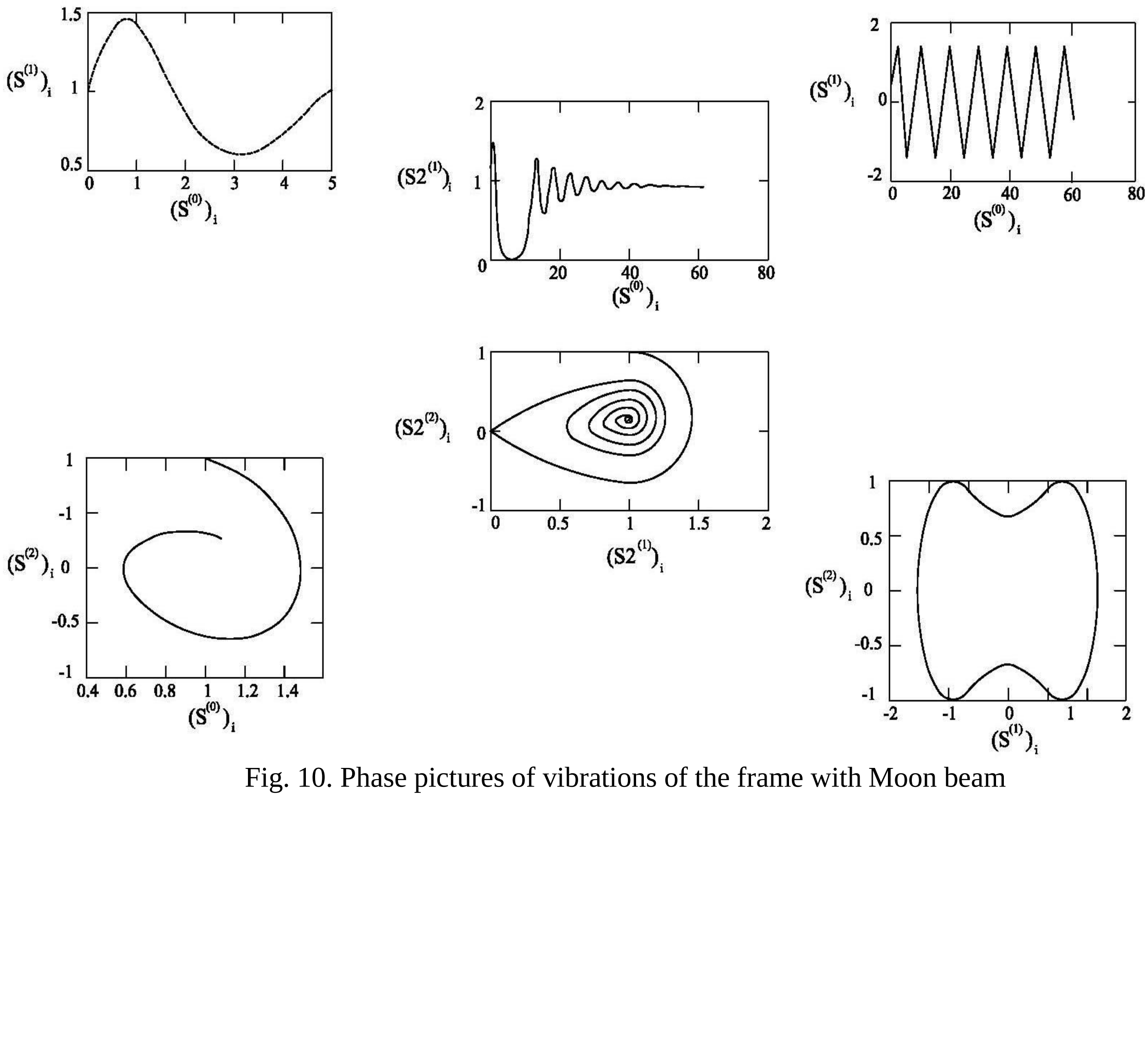

Fig. 10. Phase pictures of vibrations of the frame with Moon beam

Vibration damping in frames with combined collar-beams

Let's consider the behavior of a frame with combined collar-beam affected upon with dynamic forces of seismic and wind.

Frame with combined collar-beam consists of posts rigidly connected to collar-beam and anchored in foundation.

Combined collar-beam is presented in two versions with parallel tie-bar and strut.
It must be mentioned that parallel tie bar, as well as strut can be prestressed or stressless (Fig. 11.).

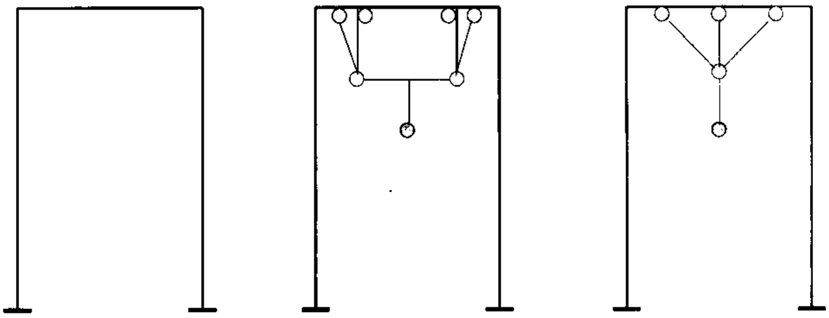

a) b) c)

Fig. 11. Frame diagrams with combined cross-bars:

a) simple frame, b) frame with combined collar-beam (tie-bar and pendulum), c) frame with combined collar-beam (strut and pendulum).

Stressless version is considered.

In both cases, parallel tie-bar, as well as, strut have load suspended in the middle, though suspension point may be in any place.

The suspended load can be considered as physical or mathematical pendulum according to the diameter of suspension tie-bar and the dimensions of load.

The behavior of mathematical and physical pendulum according to immovable suspension point have been studied thoroughly enough.

In frame system operation the maximum amplitude and pendulum vibration state are of particular interest as with consideration of nonlinearity when pendulum deviation angles are different and pendulum suspension length changes, the vibration deviation and motion stability are changed respectively which is connected with pendulum load impacts to frame posts and failure of vibration isochronism.

In order to define motion state and maximum amplitude the numerical test has been carried out with program "MATCAD-2000".

Pendulum motion equation was considered with unit frequency during 5 seconds.

When considering the analogous problem it has been noted that accuracy degradation for angles approximating $180^0(\pi)$ is regarded as critical value: at transition to this value the character of motion changes - instead of vibrations we get rotation.

The same picture is noted when investigating the equation:

$$\frac{d^2}{dt^2}\theta(t) \mp \sin\left[\theta(t)\right] = 0 \tag{30}$$

with the only difference that accuracy degradation, when determining the vibration amplitudes, began when angle of deflection got over 81^0 48'.

The example of a boundary value problem is given in Fig. 12.

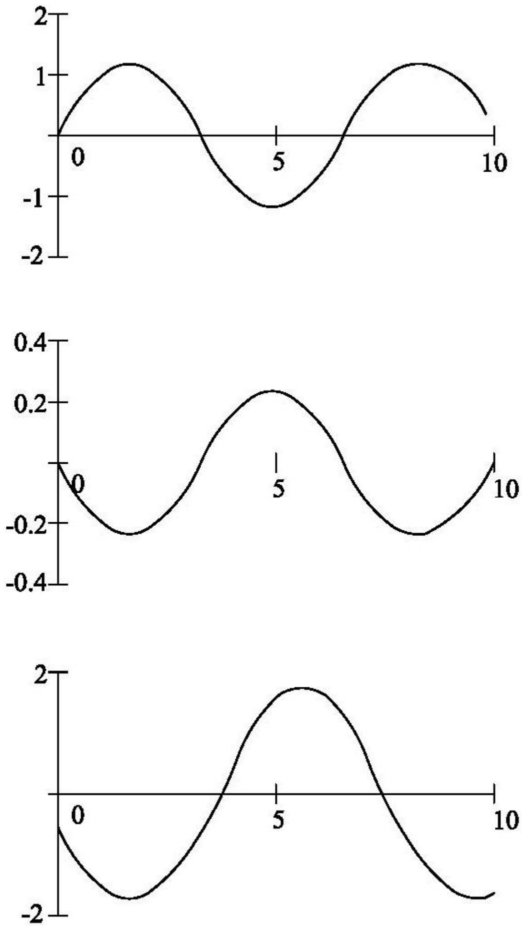

Fig. 12. Pendulum vibration at different initial angles of deflection.

At different initial angle of deviation the similar length pendulums vibrate with different amplitudes but the periods of their vibrations will be similar if pendulum deviation angle does not exceed several degrees (1÷3)

The amplitude of vibrations of one pendulum will be more, that of another will be less, but amplitude duration for both pendulums will be similar. This is the peculiarity of the phenomenon of pendulums isochronous vibration. But as it is seen from numerical experiment this phenomenon at large deflection of angles is infringed and this is to be considered at frame system operation when suspended pipelines or suspended pendulums are used as frame vibrations dampers.

In this case the point of suspended pendulum anchoring is not fixed and makes periodical horizontal and vertical movements.

For the analysis of joint operation of parallel tie-bars and suspended pendulum under dynamic action the separated or independent method can be used.

Differential equation of parallel tie-bar motion in air flow can be expressed with Duffing equation:

$$m\ddot{y} + a_1 y + a_3 y^3 = P(t) \tag{31}$$

where P(t) is Carman's exciting force:

$P(t)=0,5\rho v^2 C_R S \sin\theta t$

$$a_1=4H/l;\ a_3=8EF/l^3$$

Here H is a bunton in tie-bar;
l is brace length;
EF is brace rigidity;
ρ is air density;
v is air flow rate;
C_R is total aerodynamic coefficient:

$$\theta = Sh \cdot v / d$$

Sh is Strouhal number;
d is brace cross-section.

The amplitude of induced vibrations of the brace is determined from the following expression:

$$A^3 + A\left(\bar{\omega}^2 - \theta^2\right)\frac{3}{4h} - \frac{2}{3h}\rho V^2 C_R S = 0 \tag{32}$$

where h=8EF/Ml^3

M is brace mass.

Lateral oscillations of brace change the location of gravity center of physical pendulum (Fig. 13).

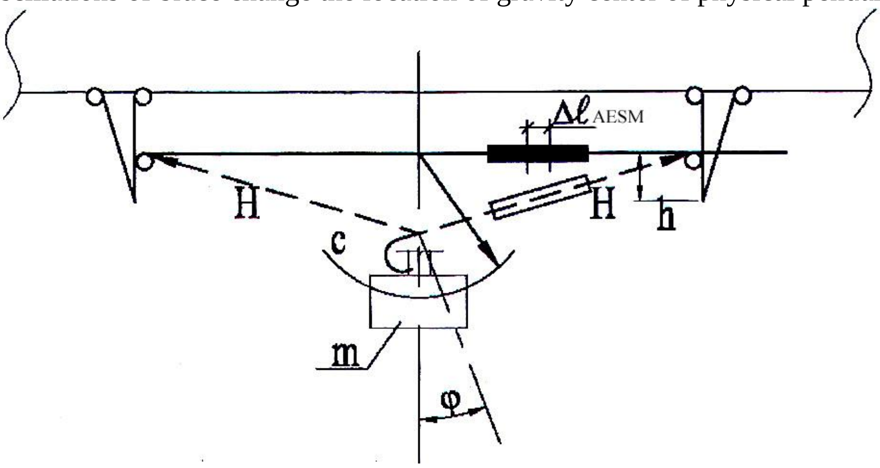

Fig. 13. Diagram of parallel brace (brace and pendulum).

Kinetic and potential energy of physical pendulum will be:

$$T = 0{,}5I\varphi^2 \quad v = v_1 + v_2$$

$$v_1 = 0{,}5C\frac{r}{R}\varphi^2; \quad v_2 = m(R+y)(1-\cos\varphi)g$$

where

I is inertia moment of physical pendulum;

C is the stiffness of physical pendulum suspension;

g is free fall acceleration;

r is the height of suspension;

R is gravity center height of physical pendulum;

y is ordinate.

The second order Lagrange equation has the following form:

$$\frac{d}{dt}\left(\frac{\partial T}{\partial \dot{q}_r}\right) - \frac{\partial T}{\partial q_r} + \frac{\partial v}{\partial q_r} = Q_r \tag{33}$$

If suppose that Q_r=0, we get system motion equation with periodical coefficients:

$$\frac{\partial^2\varphi}{\partial t^2} + \omega_0^2\left(1 - \mu\cos\bar{\omega}t\right)\varphi = 0 \tag{34}$$

where

$$\omega_0 = \frac{cr}{IR} + \frac{mgh}{I}$$

$$\bar{\omega}^2 = \omega^2 - \frac{3}{4}hA^2;$$

$$\mu = mgA / I\omega_0^2$$

Here A is amplitude which is received as a result of solution of brace equation.

As it is known the first area of instability for Mathieu equation is determined from inequality:

$$1 - \frac{1}{2}\mu + \cdots \le \frac{4\omega_0^2}{\bar{\omega}^2} \le 1 + \frac{1}{2}\mu\cdots \tag{35}$$

The effect of a cross-bar combined of brace and suspended pendulum on the operation of frame system under dynamic action of wind and seismic is consider on example of single span, one storey steel frame with the following initial data:

Frame span - L=3,0m;
Frame height – H=5,0m
Frame beam and columns made of pipes with section diameter – 140X140mm;
Brace with cable diameter – 12,0mm;
Pendulum suspension with cable diameter – 12.0 mm;
Pendulum weight: G=2400 kg.

Brace anchors are located in the distance of 0.5 m from frame joint. Seismic action is 8 points of MSK-64.

The frequency of frame natural vibrations in the first form for simple frame is 5.995 Hz (period 0.167 sec). The joint point of cross-bar and column has displaced horizontally for 0.004467 m.

The variation of frame joint displacement because of load in horizontal direction for simple systems is of linear dependence.

The frequency of natural vibrations of a frame with strut and pendulum made, by the first form, 5.932 Hz and maximum amplitude, by the first form, is 0.004586 m. For that with parallel braces maximum amplitude is 0.001838 m.

Calculation was performed using programs “LIRA” and “MIRAZH”.

As a result of carried out numerical modeling (Table 2) for investigation of frame dynamic behavior we conclude that using brace and suspended pendulum, dynamic characteristics in frame systems, particularly frequency (period) and vibration amplitude can be significantly varied.

The best result is received when vibration amplitude decreases 2.4 times. At the same time nonlinear behavior of a pendulum (magnitude of deflection angle), as well as united vibrations of brace and pendulum and their vibrations within stability areas effect the regulation of dynamic characters in frame system.

Table 2

The results of numerical modeling

№ Load	№ Mode	Eigenvalue	Frequency		Period
			rad/sec	1/sec	
2	1	0,027	0,027	37,666	0,167
2	2	0,016	0,016	62,569	0,100
2	3	0,009	0,009	111,939	0,056

Frame systems with diagonal bracing and dampers placed on them

In the practice of railway electrification rigid cross-pieces (cross-bar anchoring supports) are used for getting anchor forces of different contact wires.

The supports of power lines also have the frame structure form with suspension insulator strings of power lines.

Frame supports are used for suspension of pipelines in one and two storey single span frames.
The span structure of suspended bridges is also suspended on portal frames with pendulum type vibration dampers installed in constructions. In the supports of power lines and suspended pipe lines besides Π-shaped frames there are used the A-shaped frames as well.

Frame system with diagonal bracings and pendulum is a complex system consisting of two separate systems: frame construction itself and diagonal bracings connected to each other with a pendulum.

Here, the word “bracing” means that the vibrations of one system affect another system and vice versa.

For physical analysis of the phenomenon in a complex system it is necessary to know the nature of vibrations in separate “partial” systems which make the complex system.

Partial system is received from a complete system when we have “rigid” anchoring of all joints except the given one.

In the considered case such limitation was done to the frame. Diagonal bracings with pendulum vibrate in drawing plane, as well as horizontally to drawing plane.

Consider two frame systems with diagonal bracings and pendulum: the first frame with symmetrical diagonal bracings and suspended pendulum in the middle of frame beam. The second with pendulum suspended in equal distances from upper joints of frame (Fig. 14a, b).

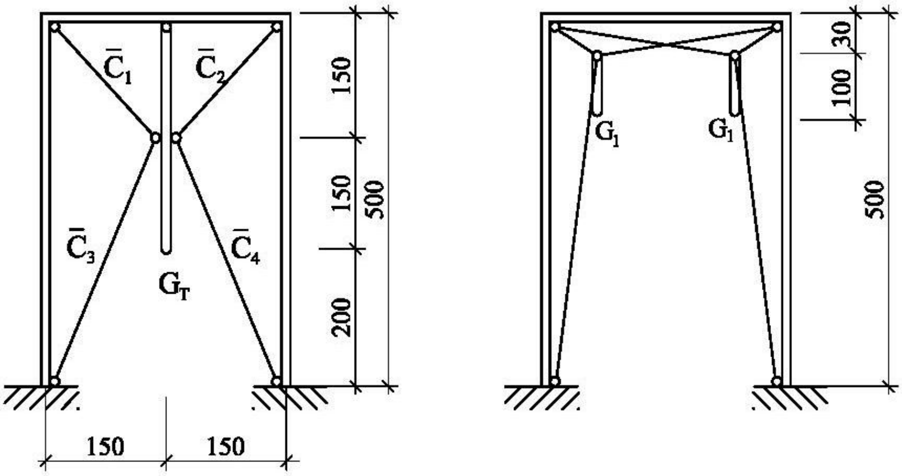

Fig. 14. Diagram of a frame with symmetrical diagonal bracings and pendulums.

Frame systems can vibrate longitudinally, as well as laterally to frame plane.

Motion equation of the pendulum with diagonal bracings

The diagram of diagonal bracings with pendulum is given in Figs. 15 and 16.

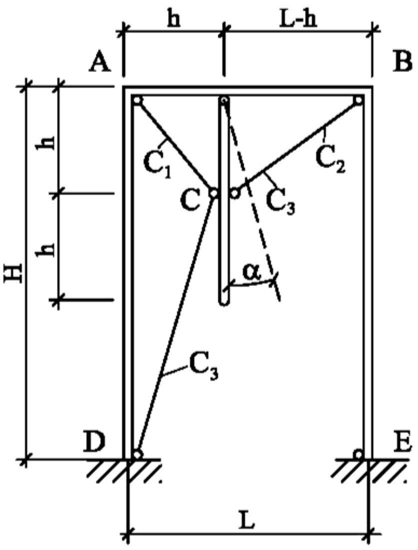

Fig. 15. General view of a frame with asymmetric diagonal bracings and pendulum.

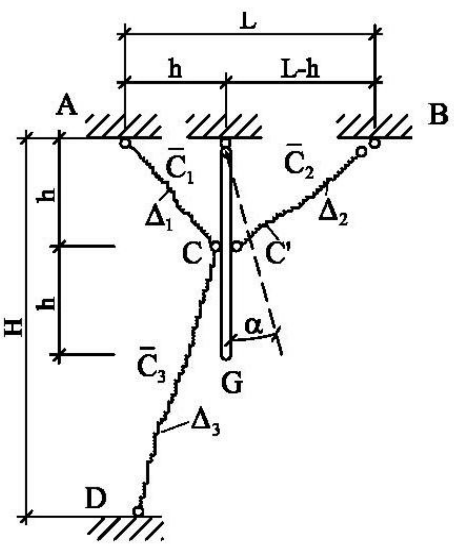

Fig. 16. Design scheme of diagonal bracings and pendulum.

Potential energy of the system is:

$$\sum \ddot{I} = \ddot{I}_1 + \ddot{I}_2 + \ddot{I}_3 + \ddot{I}_{iayo} = \frac{\bar{N}_1\Delta_1^2}{2} + \frac{\bar{N}_2\Delta_1^2}{2} + \frac{\bar{N}_3\Delta_1^2}{2} + G\Delta h \qquad (36)$$

$$\ddot{I}_{iayo} = G\Delta h = G\left(h - h\cos\alpha\right) \qquad (37)$$

Kinetic energy of the system is:

$$\dot{O} = \frac{1}{2}\frac{G}{g}h^2 \cdot \alpha^2 + \frac{1}{2}\cdot\frac{1}{3}\frac{G}{g}h^2 \cdot \alpha^2 \qquad (38)$$

Use the theorem of cosines (Fig. 17):

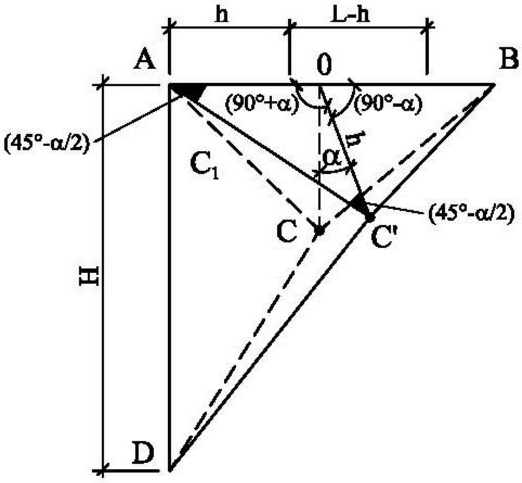

Fig. 17. Geometrical diagram of bracings.

$$\left(AC'\right) = h^2 + h^2 - 2h\cdot h\cos\left(90° + \alpha\right)$$

$$\left(BC'\right) = h^2 + \left(L-h\right)^2 - 2h\cdot\left(L-h\right)\cos\left(90° - \alpha\right)$$

$$\left(DC'\right) = H^2 + \left(AC'\right)^2 - 2H\left(AC'\right)\cos\left(45° + \frac{\alpha}{2}\right)$$

The increment of bracing lengths is:

$$\Delta_1 = AC' - AC = \sqrt{h^2 + h^2 - 2h\cdot h\cos\left(90° + \alpha\right)} - \sqrt{2}\cdot h$$

$$\Delta_2 = BC - BC' = \sqrt{\left(L-h\right)^2 + h^2} - \sqrt{h^2 + \left(L-h\right)^2 - 2h\left(L-h\right)\cos\left(90° - \alpha\right)}$$

$$\Delta_3 = DC' - DC = \sqrt{H^2 + \left(AC'\right)^2 - 2H^{(AC')}\cdot\cos\left(45° + \frac{\alpha}{2}\right)} - \sqrt{\left(H-h\right)^2 + h^2}$$

Second degree Lagrange equation:

$$\frac{d}{dt}\left(\frac{\partial T}{\partial \dot{q}}\right) - \frac{\partial T}{\partial q} + \frac{\partial \ddot{I}}{\partial q} = Q$$

for natural oscillations: Q=0, here $\frac{\partial T}{\partial q} = 0$.

Determination of derivatives of potential and kinetic energy:

$$\ddot{I}_{iayo} = G\Delta h = G\left(h - h\cos\alpha\right)$$

$$\frac{\partial \ddot{I}_{iayo}}{\partial \alpha} = Gh\sin\alpha$$

$$T = \frac{2}{3}\frac{G}{g}h^2 \cdot \alpha^2; \quad \frac{\partial T}{\partial \alpha} = \frac{4}{3}\frac{G}{g}h^2\left(\frac{d^2\alpha}{dt^2}\right)$$

$$\frac{\partial \ddot{I}_{iayo}}{\partial \alpha} = \frac{\partial}{\partial \alpha}\left(\frac{\bar{N}_1\Delta_1^2}{2} + \frac{\bar{N}_2\Delta_1^2}{2} + \frac{\bar{N}_3\Delta_1^2}{2}\right) + G\Delta h\sin\alpha$$

The equation of motion of partial system with damping taken into consideration, has the following form:

$$\frac{d^2\alpha}{dt^2} + \varepsilon\frac{d\alpha}{dt} + \omega^2\alpha + \xi\alpha^2 + \beta\alpha^3 + \gamma\alpha^5 + P = 0 \tag{39}$$

where ω^2 is the frequency of natural oscillations of the partial system;

ξ, β, γ are nonlinearity coefficients of the system;

P is the free member;

ε is the coefficient of damping.

The frequency of natural oscillations is determined with formula:

$$\omega^2 = a_1 + a_2 + a_3 + a_4 + a_5 = \sum_{i=1}^{i=5} a_i \tag{40}$$

where

$$a_1 = \frac{3g}{4h}$$

$$a_2 = \frac{3}{8}\frac{g\bar{C}_1}{G}$$

$$a_3 = \frac{3g}{4Gh^2}\frac{\overline{C_2}}{2}\frac{16h^4\left(L-h\right)}{\left(4h^2 + L^2 - 2Lh\right)^2}$$

$$a_4 = \frac{3g}{4Gh^2}\frac{\overline{C_3}}{2}\left(\frac{h^2}{2} - \frac{3Hh}{4}\right)\left[1 - \frac{\left(H^2 + 3h^2 - 2Hh\right)}{2h\left(H^2 + 2h^2 + 2Hh\right)^{1/2}}\right]$$

$$a_5 = \frac{3g}{4Gh^2}\frac{\bar{C}_3}{2}\left[\frac{8h^4}{4\left(H^2 + 2h^2 + 2Hh\right)}\right]$$

In particular case when $\bar{C}_1 = \bar{C}_2 = C$ and $\bar{C}_3 = \bar{C}_4 = 0$ the frequency of natural oscillations of the frame with bracings and pendulum equals:

$$\omega = \sqrt{\frac{3g}{4}\left(\frac{C}{G} + \frac{1}{h}\right)} \tag{41}$$

which coincides with the presented expression.

Numerical example

For example consider two diagrams of the frame with diagonal bracings and pendulums (see Fig. 14 a,b).

Initial geometrical data are given in Fig. 14 a,b for diagram. The frame is made of pipes with diameter D = 140 mm and wall thickness t = 36 mm, diagonal bracings are plain reinforcement with diameter D = 12 mm, suspended pendulum is of round steel with diameter D = 32 mm, load at the end G = 12500 kg. The coefficient of stiffness of diagonal bracings is:

$$\bar{C}_1 = \bar{C}_2 = 10670 kg/sm; \; \bar{C}_3 = \bar{C}_4 = 5953 kg/cm$$

For the diagram given in Fig. 14b the frame is made of pipes with diameter D = 140 mm and wall thickness t = 40 mm. Diagonal bracings and pendulum suspension are made of cable with diameter D=12.0 mm.

On the end of suspended pendulum the loads, each weighting G = 2400 kg, are located.

The calculation of the first diagram was done in program SAP 2000. The vibrations of frame system happened vertically to frame plane.

The first period of natural vibrations of frame system in the first mode was T = 0.4456 sec.

Without diagonal bracings and pendulum and with the load in the middle of frame cross-piece the oscillation period made T = 0.4410 sec.

Hence, the existence of diagonal bracings with suspended pendulum changes the period of frame system natural oscillations for 7.4 %.

The first mode of frame system vibrations is given in Fig.

The calculation of the second diagram is performed in program "LIRA-8.2".

The comparison of vibration amplitudes (in drawing plane) to a simple frame and a frame with diagonal bracings and two pendulums showed that in the first case the deviation was 4.467 cm and in the second case – 0.148 cm.

For simple frame the vibration period in the first mode is T = 0.167 sec. For the frame with diagonal bracings and pendulum T = 0.7 sec. The difference made 76 % (Fig.).

Thus, it can be concluded that for damping of vibrations in frames the diagonal bracings with suspended loads (pendulum type) can be successfully used which significantly changes the frequency of vibrations (period) and decreases amplitudes.

Experimental research of steel frames with combined dampers

In order to continue earlier carried out test researches for static and dynamic effects the steel frame have been experimentally investigated. Frame operation was studied in two ways: by physical and computer modeling, which have two types of dampers: combined dampers with horseshoe-shaped devices and round link dampers.

Test model (Fig. 18, 19, 20, 21, 22) represents a closed type frame made of tubular members with D = 34 mm, pipe wall thickness t = 3.5 mm, The dimensions of frame model are: span l = 55.0 cm; frame height h = 122.0 cm; distance from frame support to its first collar-beam - 9.0 cm. Inside the frame a damper with two types of bracings is located.

The first type of a damper is a horseshoe circle with diameter - 15.3 cm, thickness - 6.0 mm and width 2.5 cm. The clearance in the circle is 3.0 cm.

Bracings are made of cables of 1.8 mm diameter.

The horseshoe circle is fixed in the middle of collar-beam with rubber pod using shock absorber. A trussed construction is installed in 16.0 cm from the upper collar-beam of the frame.

The second type of a damper represents a closed circle with diameter - 15.3 cm, thickness - 6.0 mm and width 2.5.cm. The circle is installed in the middle of frame span on the half height of the frame. In four points of the circle bracings of diameter 1.8 mm are fixed in diagonal direction.

On the upper collar-beam of frame model an electric motor with load is mounted. In the upper joint of the frame static load P = 120-140 daN (1 daN –decaneuton = 1 kgf) is applied with the help of horizontal cable and with the use of dynamometer.

Fig. 18 View of experimental model of the frame with ring bracing.

Fig. 19. Used measuring device.

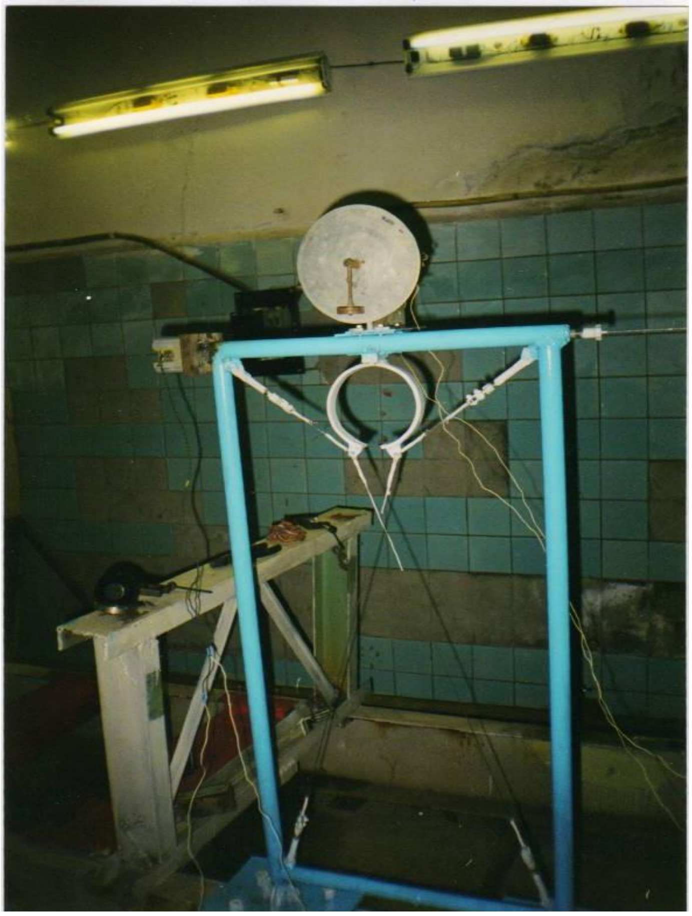

Fig. 20 View of experimental model of the frame with horseshoe-shaped bracing.

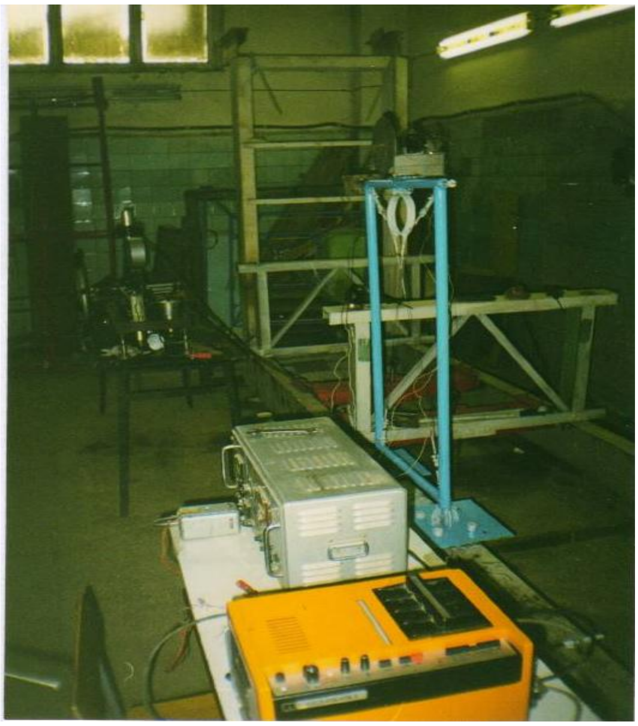

Fig. 21. Used measuring device.

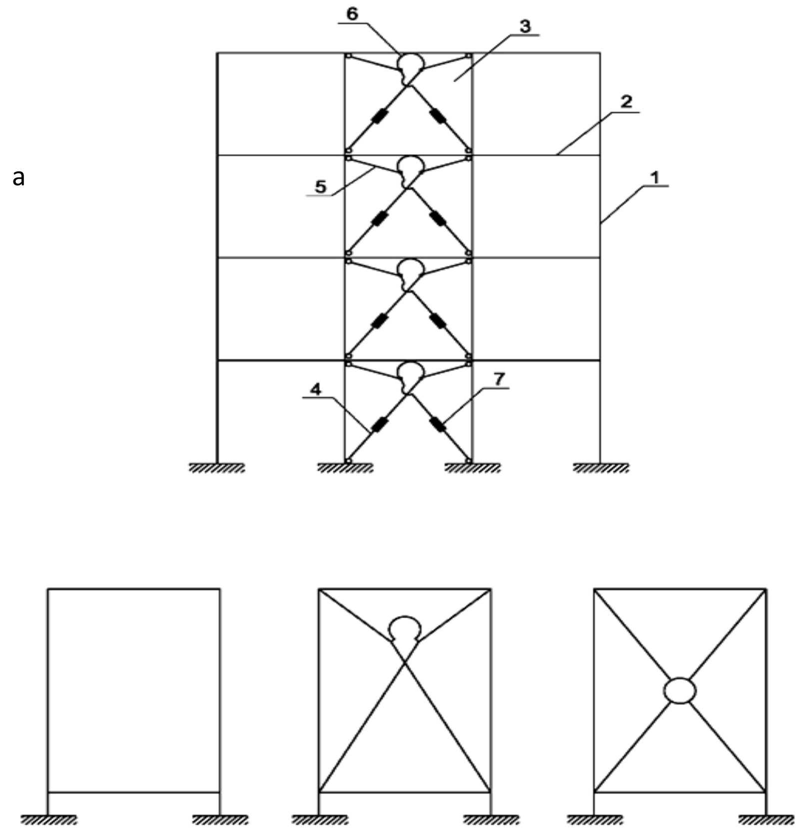

Fig. 22 Diagrams of frame test models with combined dampers of vibrations.

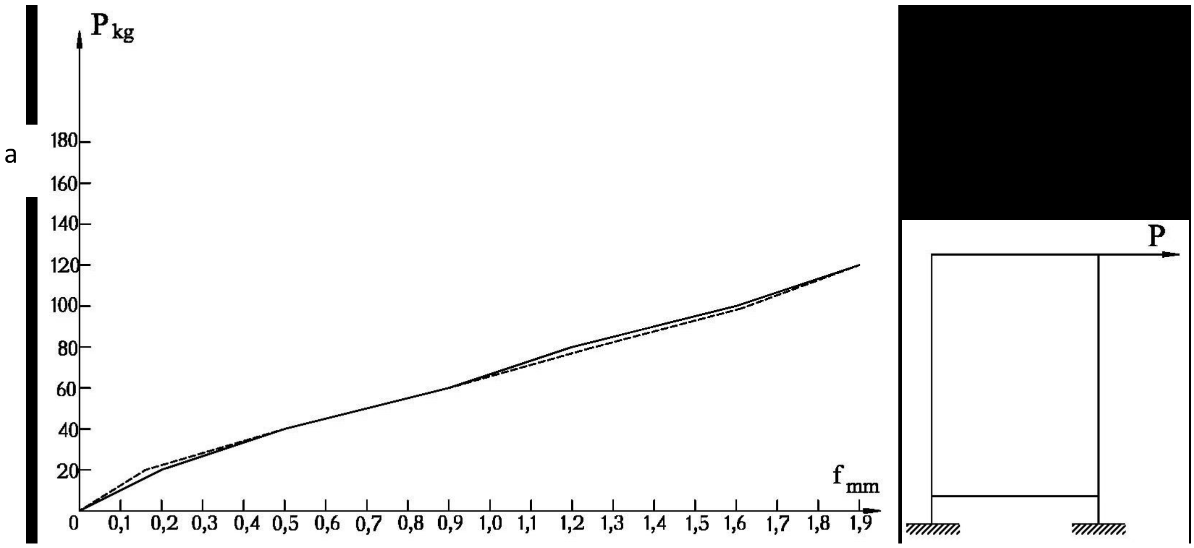

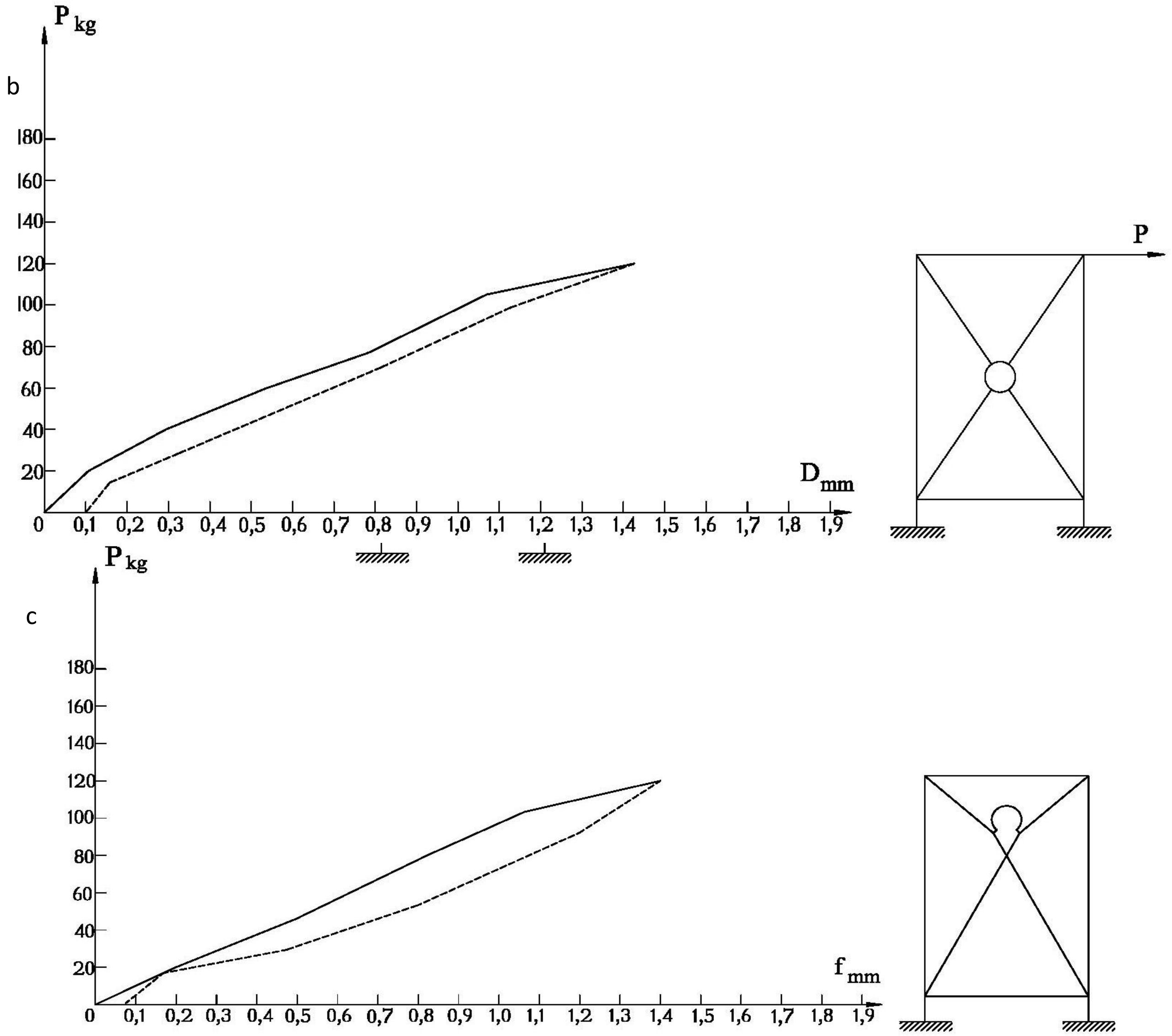

Fig. 23. Graph of frame displacement: ——— loading - - - - -unloading.

Static loading in joint was transmitted step-by-step with 20 decaN (six steps in all) and horizontal displacement of frame was measured with Macsimov's deflection meter. Readings are given in the form of a table.

Dynamic loading of frame was done with electric motor with eccentrically arranged load. The registration of vibrations was done with oscillograph HO441 and vibro-sensor KH001Г.

The number of electric motor revolutions was registered with tachometer ИO-30.

Vibrations were recorded on paper film with time mark of 0.1 sec.

Vibrations were recorded under static load applied in the upper joint of the frame P = 60 daN and in case of bracings tension equal to 50 daN.

The frequency of forced oscillations made θ=18 sec. The results of processing of oscillograph records are given in the Table.

Computer modeling of frame with combined damper is accomplished in programs SAP-2000" and "LIRA-8".

While using the both programs the horizontal load P = 150 daN applied in the upper joint of the frame is considered. The horizontal cable as well as horizontal bracing of upper joint is not taken into account.

Therefore, the values of frame system periods and dynamic displacements differ from experimental data and only their qualitative part is preserved and enables to estimate the effect using.

As a result of tests and computer modeling it can be concluded that using of two types of dampers in frames significantly change vibration periods and decrease dynamic displacements.

Compared to the usual frame the coefficient of amplitude decrease without damper is K = 1.14 for circular damper and K = 1.18 for horseshoe damper, i.e. frame oscillation amplitude decreases for 18 % (Table 3).

Table 3

Frame displacement caused by static load (Fig. 23 a,b,c, d,e)		Coefficient of frame oscillation amplitude reduction caused by dynamic load	
Frame designation	Δ mm	Frame designation	K
Simple frame	1.9	Simple frame	1.0
Frame with circular damper	1.35	Frame with circular damper	1.14
Frame with horseshoe damper	1.38	Frame with horseshoe damper	1.18

Regulation of strains of prestressed beams

Generally collar-beams are fixed to frame columns jointly and rigidly (Fig. 25). Joint support of the collar-beam on frame columns enables to consider it as the girder supported on two supports with prestressed parallel tie-bar on which AЭСМ is mounted (Fig. 26, 27).

Double-T beam loaded with static load is taken as prestressed steel girder.

The displacement of not preliminarily tensioned beam as a result of uniformly distributed and concentrated loads is expressed with formula:

$$f = \frac{5}{384}\frac{q^{\sigma}\ell^{4}}{E\Im} + \frac{P^{\sigma}\ell^{3}}{48E\Im} \qquad (42)$$

Here q^{σ} is equdistributed standard load per one meter of girder;

P^{σ} is concentrated standard load;

ℓ beam span;

$\Im$ inertia moment of the girder;

E is module of flexibility.

Double-T beam is I N 16 (cross-section area A = 20.0 cm^2, $\Im$=873cm^4; q^{σ}=15daN/m; R_y=2100daN/cm^2; E=2100000 daN/cm^2).

1daN = 10 N = 1 kg is taken as dimension.

Freely supported beam span l = 324 cm.

The displacement of prestressed beam because of static load can be expressed with the following approximated formula:

$$f = \frac{1}{48E\Im}\left(p^{\sigma}\ell^{3} + \frac{5}{8}q^{\sigma}\ell^{4} - 6\left(X_1 + X_2\right)\bar{h}\ell^{2}\right) \qquad (43)$$

Here X_1 and X_2 are prestressed and selfstrain forces;

$\bar{h}$ is the distance from guy-rope axis to neutral axis.

Test model of steel beam represented a double-T beam I N16, steel =st.3; parallel tie-bar with diameter Ø2.1 mm, length of cable-tie bar L = 1600 mm; beam span l = 3240 mm.

In the middle part of the beam on its upper shelf an electric engine was mounted.

Static displacements and vibration amplitudes were measured with Maksimov’s deflection meter.

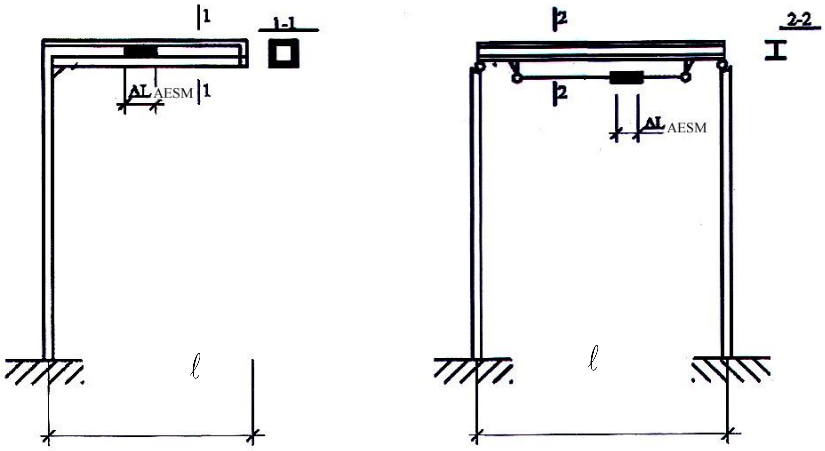

Fig. 24 Diagrams of prestressed frames

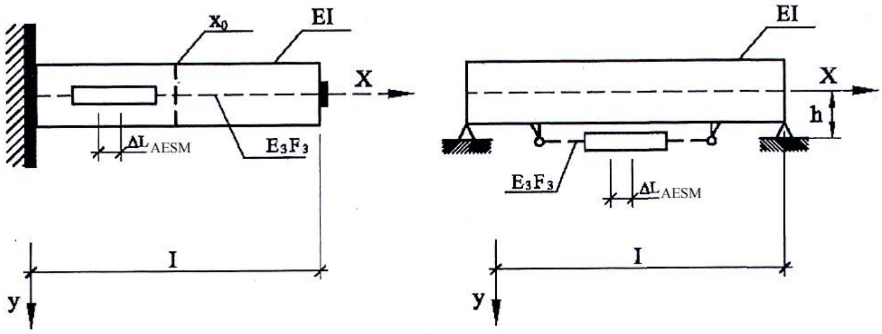

Fig. 25 Diagrams of prestressed frames

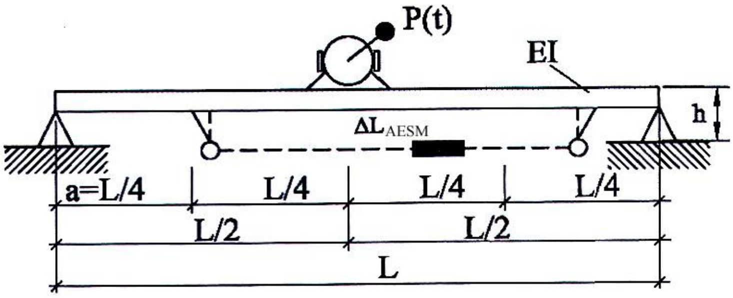

Fig. 26 Diagrams of prestressed beam under dynamic load

Concentrated load is applied step-wise in the middle part of the beam and when tension in brace and beam displacement were measured achieved 500 daN (5.0 kN).

When static concentrated load achieved P = 500 daN (5.0 kN) and tension in the tie-bar achieved S = 105 daN (1.05 kN) the displacement in the middle part of the beam made 0.9 cm, unstrained beam displacement made 1.2 cm. The decrease of displacement was 8.0 – 25% (Fig. 28, 29, 30, 31, 32).

Here "MMA" means Macsimov's apparatus, "IND" – indicator-deflectometer

The exact expression for the curve of a beam or a column is:

$$\chi = \qquad (3.44)$$

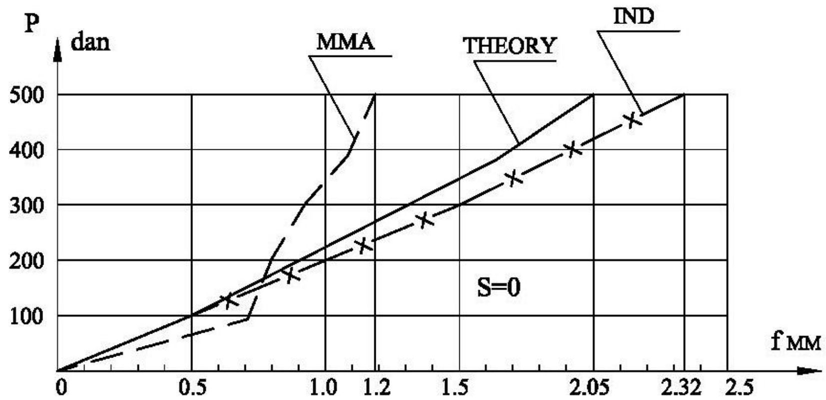

Fig. 27 Diagrams of theoretical and experimental results of deflections, S=0.

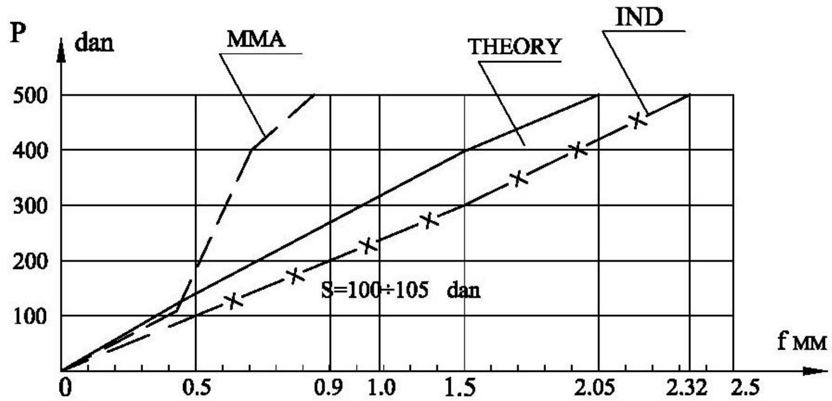

Fig. 29 Diagrams of theoretical and experimental results of deflections, S=100÷105daN.

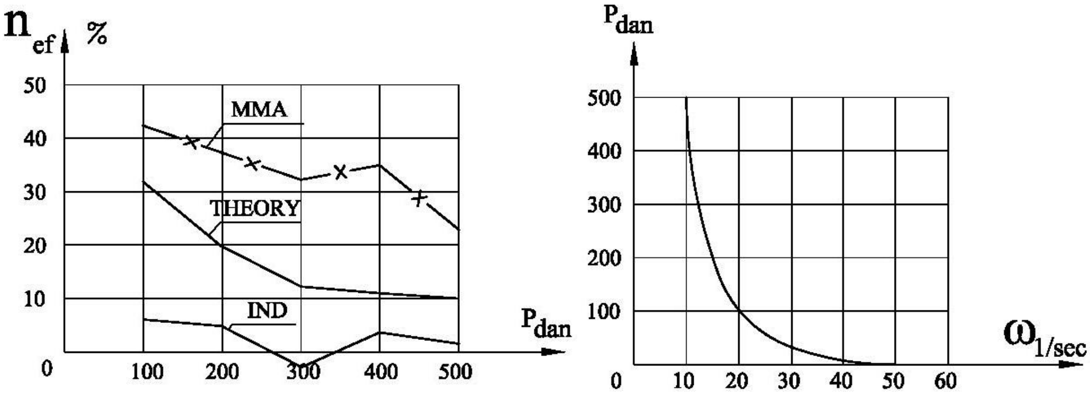

Fig. 30. Efficiency of beam prestressing for deflection and natural vibration frequency.

Hence we get

$$E\Im(x)\frac{d^4y}{dx^4} = q(x) \tag{44}$$

With concentrated forces taken into consideration:

$$E\Im(x)\frac{d^4y}{dx^4} = q(x) + \sum_{i=1}^{i=n} P_i\delta\left(x-a_i\right) + \sum_{i=1}^{i=n} M_i\delta'\left(x-b_i\right) + \cdots \tag{45}$$

where δ is delta function.

In our case we shall have the following expression:

$$E\Im(x)\frac{d^4y}{dx^4} = q(x) + P(t)\delta\left(x-a\right) + M(t)\delta'\left(x-b\right) - M(t)\delta'\left[x-(\ell-b)\right] \tag{46}$$

Using d'Alembert principle from static equation we get dynamic equation:

$$E\Im(x)\frac{d^4y}{dx^4}=\bar{m}(x)\frac{\partial^2 y}{\partial t^2}+\bar{M}\delta(x-a)\frac{\partial^2 y}{\partial t^2}=P(t)\delta(x-a)+M(t)\delta'\left(x-b\right)-M(t)\delta'\left[x-(\ell-b)\right] \quad (47)$$

Time dependent factors:

$$P(t)=P_0\cos\omega t;\quad \mathrm{M(t)=M_0}\cos\omega t$$

$$y(x,t)=W(x)\cos\omega t;\quad \mathrm{y}^{IV}=W^{IV}(x)\cos\omega t$$

$$\text{and } \ddot{y}=-\omega^2W(x)\cos\omega t$$

If we substitute equations into 47, we get:

$$\frac{d^4W(x)}{dx^4}\cos\omega t-\frac{m(x)}{E\Im(x)}\omega^2W(x)\cos\omega t-\frac{\bar{M}}{E\Im(x)}\delta(x-a)\omega^2W(x)\cos\omega t=$$
$$=P_0\delta(x-a)\cos\omega t+M_0\delta'\left(x-b\right)\cos\omega t-M_0\delta'\left[x-(\ell-b)\right]\cos\omega t \quad (48)$$

Accept the solution of equation (48) as $W(x)=f\sin\frac{\pi x}{\ell}$ with boundary value conditions satisfied:

$$x=0;\quad \mathrm{W(x)=0}$$
$$x=\ell;\quad \mathrm{W}(\ell)=0 \quad (49)$$

If we use Bubnov-Galerkin method and determine:

$$\frac{d^4W}{dx^4}=f\frac{\pi^4}{\ell^4}\sin\frac{\pi x}{\ell}$$

we get:

$$\int_0^\ell f\frac{\pi^4}{\ell^4}\sin\frac{\pi x}{\ell}\sin\frac{\pi x}{\ell}dx-\int_0^\ell\frac{\bar{m}(x)}{E\Im(x)}\omega^2 f\sin\frac{\pi x}{\ell}\sin\frac{\pi x}{\ell}dx-$$
$$-\int_0^\ell\frac{\bar{M}(x)}{E\Im(x)}\omega^2 f\delta(x-a)\sin\frac{\pi x}{\ell}\sin\frac{\pi x}{\ell}dx=\int_0^\ell\frac{P_0}{E\Im(x)}\delta(x-a)\sin\frac{\pi x}{\ell}dx+ \quad (50)$$
$$+\int_0^\ell\frac{M_0}{E\Im(x)}\delta'(x-a)\sin\frac{\pi x}{\ell}dx-\int_0^\ell\frac{M_0}{E\Im(x)}\delta'\left[x-\left(\ell-b\right)\right]\sin\frac{\pi x}{\ell}dx$$

After integration when $E\Im(x)=const$ and $\bar{m}(x)=const$, we get:

$$f\frac{\pi^4}{\ell^4}\frac{l}{2}-f\frac{\bar{m}}{E\Im}\omega^2\cdot\frac{\ell}{2}-f\frac{\bar{M}}{E\Im}\omega^2\cdot 1=\frac{P_0}{E\Im}\cdot 1-\frac{M_0}{E\Im}\frac{\pi}{\ell}\cos\frac{\pi b}{\ell}+\frac{M_0}{E\Im}\frac{\pi}{\ell}\cos\frac{\pi(\ell-b)}{\ell} \quad (51)$$

or

$$f\left(\frac{\pi^4}{2\ell^3}-\frac{\bar{m}\omega^2\ell}{2E\Im}-\frac{\bar{M}\omega^2}{E\Im}\right)=\frac{P_0}{E\Im}-\frac{M_0}{E\Im}\frac{\pi}{\ell}\frac{\sqrt{2}}{2}-\frac{M_0}{E\Im}\frac{\pi}{\ell}\frac{\sqrt{2}}{2} \quad (52)$$

Here $M_0=\frac{E_sF_s\bar{h}_s}{L_s}\Delta\ell_{AESM}$;

s index belongs to brace;

$E_s F_s$ is brace rigidity including AESM.

and hence we have:

$$f=\frac{\frac{P_0}{E\Im}-\frac{\pi\sqrt{2}M_0}{E\Im\ell}}{\frac{\pi^4}{2l^3}-\frac{\bar{m}\omega^2\ell}{2E\Im}-\frac{\bar{M}\omega^2}{E\Im}} \quad (53)$$

After solving the equation of motion (eq. 3.48) we define the gap between contactors with AESM device:

$$\Delta\ell_{A\text{Э}CM}=\left[2P_0\ell^3L-fL\left(\pi^4E\Im-\bar{m}\omega^2\ell^4-2\bar{M}\omega^2\ell^3\right)\right]/\,2{,}82\pi E_sF_s\bar{h}_s\cdot\ell^2 \quad (54)$$

where P_0 is concentrated force on tie;

f is the amplitude of tie vibration;
ℓ is tie span;
L is tie-bar length including AESM;
$\bar{m}$ is uniformly distributed mass on the tie;
$\bar{M}$ is concentrated mass on tie;
E_sF_s is tie-bar rigidity by AESM;
$\bar{h}_i$ is the distance from tie-bar axis to tie axis;
$\omega = \frac{2\pi}{T}$ is the frequency of natural vibrations of a beam which defined with formula:

$$\omega^2 = \frac{E\Im \cdot R_{1x}}{\bar{m}R_{5x} + \bar{M}R_{7x}} \tag{55}$$

where

$$R_{1x} = \int_0^\ell \frac{d^4W(x)}{dx^4} W(x)dx; \quad R_{5x} = \int_0^\ell W^2(x)dx; \quad R_{7x} = \int_0^\ell \delta(x-a)W^2(x)dx; \tag{56}$$

When $W(x) = \sin\frac{\pi x}{\ell}$, we get:

$$\omega^2 = \frac{\pi^4}{2\ell^3(0,5+\mu)} \cdot \frac{E\Im}{\bar{m}\ell}; \quad \mu = \frac{\bar{M}}{\bar{m}\ell}; \tag{57}$$

or

$$\omega = \sqrt{\frac{48,606}{(0,5+\mu)} \cdot \frac{E\Im}{\bar{m}\ell^4}} \tag{58}$$

With consideration of axial force:

$$\omega^2 = \frac{E\Im\pi^4 - N\pi^2\ell^2}{2(0,5+\mu)\bar{m}\ell} \tag{59}$$

By J.W. Rayleigh formula:

$$\omega = \sqrt{\frac{48,0}{(0,485+\mu)} \cdot \frac{E\Im}{\bar{m}\ell^4}} \tag{60}$$

By E. Sekhniashvili formula:

$$\omega = \sqrt{\frac{49,15}{(0,504+\mu)} \cdot \frac{E\Im}{\bar{m}\ell^4}} \tag{61}$$

Without concentrated mass (3.58 and 3.59), we have:

$$\omega = \frac{9,86}{\ell^2}\sqrt{\frac{E\Im}{\bar{m}}}$$

By E. Sekhniashvili formula:

$$\omega = \frac{9,875}{\ell^2}\sqrt{\frac{E\Im}{\bar{m}}}$$

By J.W. Rayleigh formula:

$$\omega = \frac{9,948}{\ell^2}\sqrt{\frac{E\Im}{\bar{m}}}$$

From the reference-book:

$$\omega = \frac{9,8596}{\ell^2}\sqrt{\frac{E\Im}{\bar{m}}}$$

Dynamic displacements of the beam were experimentally fixed with Maksimov's deflectometer according to the opening of the sector visually; when AESM was switched in sector opening decreased 3 times when the clearance between contactors was $\Delta\ell_{AESM}$=0.5 cm.

The essence of work is to develop the principles of various self-controlled structures creation.

The objective of work is to develop the principles of smart structures creation and automatic control system development.

For achievement of objective we map out the following tasks:

1. Selection of smart sensors for study of structure state - marginal state;
2. Development of sensors layout in the structures;
3. Description of informational signals of structure's internal stresses and deformations in sensors;
4. Investigation of processing methods of signals received from structures;
5. Development of actuator system;
6. Development of "structure- smart sensor-drive" system models and carrying out of numerical experiment;
7. Development of automatic control system of self-controlled structures;
8. Development of experimental test bench and carrying out of physical experiments;
9. Analysis of obtained results and final report.